Theoretical Study of the Hydride Attack on the η^5-Cyclopentadienyltricarbonyliron Cation

David A. Brown,* Noel J. Fitzpatrick, and Peter J. Groarke

Department of Chemistry, University College, Belfield, Dublin 4, Ireland

Nobuaki Koga and Keiji Morokuma

Department of Theoretical Studies, Institute for Molecular Science,
Myodaiji, Okazaki 444, Japan

Received September 2, 1992

Various species resulting from the hydride attack on $[(\eta^5\text{-}C_5H_5)Fe(CO)_3]^+$ have been studied using ab initio molecular orbital methods at the Hartree–Fock (HF) and second order Møller–Plesset (MP2) perturbation levels. Stationary points were located and characterized for $[(\eta^5\text{-}C_5H_5)Fe(CO)_3]^+$ (I), $[(\eta^5\text{-}C_5H_5)Fe(CO)_3H]$ (II), $[(\eta^5\text{-}C_5H_5)Fe(CO)_2CHO]$ (III), $[(\eta^4\text{-}C_5H_6)Fe(CO)_3]$ (IV), and $[(\eta^3\text{-}C_5H_5)Fe(CO)_3H]$ (V). MP2 calculations showed that inclusion of dynamic electron correlation has a significant effect on the geometries and relative energies of the species considered. The final order of stabilities is IV > II ≈ III. The relative stability of the metal–formyl complex (III) correlates with its spectroscopic identification at low temperatures in the reaction of I with $NaBH_4$. Although II is of comparable stability to III, it is a weak complex between $[(\eta^5\text{-}C_5H_5)Fe(CO)_2H]$ and CO with a long Fe–CO bond (r(Fe–CO) = 4.33 Å). V is less stable than the other species resulting from hydride attack on I. Finally, the diene complex, $[(\eta^4\text{-}C_5H_6)Fe(CO)_3]$ (IV), is calculated to be the thermodynamically stable product.

Nucleophilic attack and substitution of metal carbonyl complexes is one of the longest established and most studied reactions in organometallic chemistry.[1] In the case of metal carbonyl complexes of π-acids, e.g. the title compound $[(\eta^5\text{-}C_5H_5)Fe(CO)_3]^+$, a number of reaction pathways and products may occur, including (a) addition of the nucleophile to the carbon atom of one of the carbonyl groups, (b) ring addition, (c) carbonyl substitution, and (d) breaking of the metal–ring bond with the formation of nucleophile-substituted metal carbonyls.[2,3] However, despite extensive studies, it is still difficult to make reliable predictions of either the reaction pathway or final products; indeed, these may be quite different since frequently kinetic products are observed under one set of conditions (e.g. low temperatures) and thermodynamic products under other conditions (e.g. higher temperatures). Theoretical attempts to predict the regiospecificity of such reactions have been based on Hückel theory[4] and on reactivity indices such as P_{LUMO} or the frontier electron density[5] (the density of the positive hole of the LUMO at a particular site). One of the main problems is that the simple interaction between the HOMO of the nucleophile and the LUMO of the complex, appropriate to many organic reactions, is frequently inappropriate in metal carbonyl complexes, since there is often a band of LUMOs lying quite close in energy and the interaction of the HOMO of the nucleophile with all of these must be considered. In an attempt to overcome this problem, the interaction determinant method (IDM)[6] was developed to calculate the interaction energy between an incoming nucleophile and substrate LUMOs for a particular reaction pathway and then interaction energies were compared for various sites within the substrate molecule. The problem of allowing for interaction between the HOMO of a nucleophile and a range of LUMOs as against "the LUMO" is well illustrated by the reaction between the methoxide ion and the $[(\eta^7\text{-tropyllium})Mo(CO)_3]^+$ cation.[7,8] Calculation of P_{LUMO} values indicated initial attack at a ring carbon atom whereas calculations based on either $\sum P_{\text{LUMO}}$ (summed over the band of LUMOs) or interaction energies (calculated by the IDM method) predicted initial attack at the $Mo(CO)_3$ moiety,[7] as confirmed by low temperature spectroscopic studies.[8]

Conditions such as solvent and/or nucleophile source can also influence the reactions occurring; e.g. $[(\eta^5\text{-}C_9H_7)Fe(CO)_3]^+$ reacts with $NaBH_4$ in acetone to give $[(\eta^5\text{-}C_9H_7)Fe(CO)_2CHO]$ at low temperature (−60 °C) and $[(\eta^5\text{-}C_9H_7)Fe(CO)_2H]$ and $[(\eta^5\text{-}C_9H_7)Fe(CO)_2]_2$ as the temperature increases,[9] while using $NaBH_3CN$, $[(\eta^3\text{-}C_9H_7)Fe(CO)_3H]^+$ is detected, which then forms the dicarbonyl hydride $[(\eta^5\text{-}C_9H_7)Fe(CO)_2H]$ and then the dimer, $[(\eta^5\text{-}C_9H_7)Fe(CO)_2]_2$.[10]

In this paper, we present the results of detailed ab initio calculations, at both Hartree–Fock (HF) and second order Møller–Plesset (MP2) levels, for a number of possible species which may be formed by hydride attack on the title compound, $[(\eta^5\text{-}C_5H_5)Fe(CO)_3]^+$ (I). The species considered are $[(\eta^5\text{-}C_5H_5)Fe(CO)_3]^+$ (I), $[(\eta^5\text{-}C_5H_5)Fe(CO)_3H]$ (II), $[(\eta^5\text{-}C_5H_5)Fe(CO)_2CHO]$ (III), and $[(\eta^4\text{-}C_5H_6)Fe(CO)_3]$ (IV) (Figure 1), corresponding, respec-

---

[1] Pauson, P. L. *J. Organomet. Chem.* **1980**, *200*, 207.
[2] Walker, P. J. C.; Mawby, R. J. *Inorg. Chim. Acta* **1973**, *7*, 621.
[3] Kane-Maguire, L. A. P.; Sweigart, D. A. *Inorg. Chem.* **1979**, *18*, 700.
[4] Davies, S. G.; Green, M. L. H.; Mingos, D. M. P. *Tetrahedron* **1978**, 3047.
[5] Brown, D. A.; Chester, J. P.; Fitzpatrick, N. J. *J. Organomet. Chem.* **1978**, *155*, C21.
[6] Brown, D. A.; Fitzpatrick, N. J.; McGinn, M. A. *J. Organomet. Chem.* **1985**, *293*, 235.
[7] Brown, D. A.; Fitzpatrick, N. J.; McGinn, M. A.; Taylor, T. H. *Organometallics* **1986**, *5*, 152.
[8] Brown, D. A.; Fitzpatrick, N. J.; Glass, W. K.; Taylor, T. H. *Organometallics* **1986**, *5*, 158.
[9] Ahmed, H.; Brown, D. A.; Fitzpatrick, N. J.; Glass, W. K. *Inorg. Chim. Acta* **1989**, *164*, 5.
[10] Ahmed, H.; Brown, D. A.; Fitzpatrick, N. J.; Glass, W. K. *J. Organomet. Chem.* **1991**, *418*, C14.

0276-7333/93/2312-2521$04.00/0

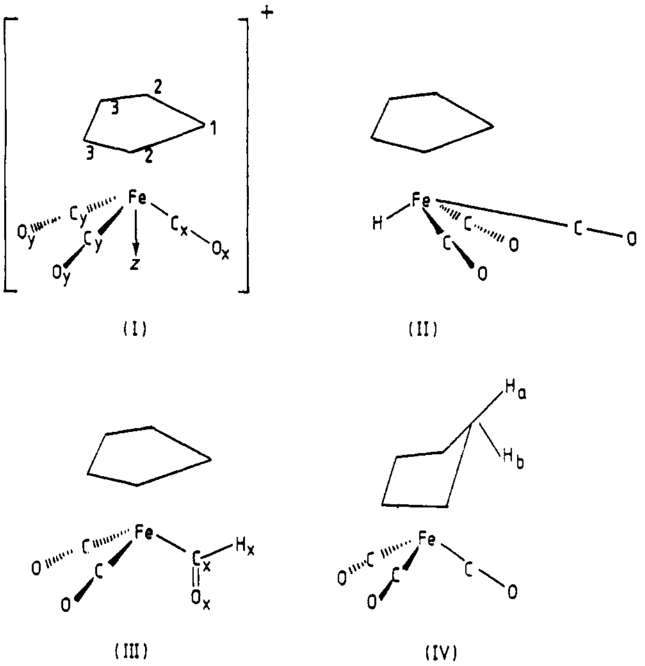

Figure 1. Species considered. In I the pseudo C_{3v} axis is equiangular with the three Fe–CO bonds. In this figure H_i is connected to C_i (i = 1–3).

tively, to the substrate cation (I), the intermediate (II) formed by direct H^- attack at the metal center, the metal–formyl species (III) formed by H^- attack at the carbonyl carbon atom, and finally the diene complex (IV), corresponding to direct ring attack. $[(\eta^3\text{-}C_5H_5)Fe(CO)_3H]$ (V) was also found as a minimum, less stable than the other species considered, II–IV.

While there have been extended Hückel studies of $[(\eta^5\text{-}C_5H_5)Fe(CO)_3]^+$ reported,[11,12] there have been no previous ab initio calculations on this species, or any of the other complexes considered in this work, published. Previous related work includes ab initio studies on $Fe(CO)_5$ and ferrocene by Almlof and co-workers[13–16] and others.[17] Ab initio studies on $H_2Fe(CO)_4$[18a] and of nucleophilic attack on the carbonyl ligand in iron carbonyl complexes have also been reported.[18b]

Method of Calculations

In the present studies, the structures of all species considered were fully optimized under the C_s symmetry constraint at the HF and MP2 levels. The assumption of C_s symmetry is discussed later. The Gaussian 90 program of Pople and co-workers was used in this study.[19] The basis set on iron, Fe(10s10p5d/4s4p2d), including p functions with exponents of 0.118 and 0.038, is due to Huzinaga et al.[20] This basis set combined with the standard split-valence 3-21G basis set on C, O, and H atoms is termed HUZ 3-21G. When the basis set of C and O is augmented by the addition of a d polarization function, with exponent 0.08, the term HUZ 3-21G* is used.

For all the species the closed-shell restricted (R) HF and restricted (R) MP2 methods were adopted. We tested, at the RMP2 structures, the stability of the RHF wave functions for I and V and found that they are stable with respect to becoming the unrestricted (U) HF wave functions. The electronic structures of II and III are expected to be similar to that of I, since all these species have the formally d^6 Fe atom. On the other hand, we found that the RHF wave function for IV with the d^8 Fe atom is unstable with respect to becoming the UHF wave function. Therefore, in addition to the RHF calculations we determined the structure of IV at the UHF level and calculated the energies for the UHF and RMP2 structures with the projected unrestricted (PU) MP2 method.

The Fe–CO and the Fe–Cp bond distances, both present in the systems studied in this paper, are known to be difficult to reproduce even qualitatively at the HF level, and much more sophisticated methods are required. Almlof et al. have found in the study of $Fe(CO)_5$ that inclusion of nondynamic electron correlation significantly improved the Fe–CO distance and that dynamic electron correlation also plays a role.[13] Ferrocene was also studied by Almlof and co-workers[14–16] using various methods as well as large basis sets. The method which reproduced most closely the observed experimental metal–ligand distance was the modified coupled pair functional method, in which all 66 valence electrons were correlated. In this method the reference wave function is a single Slater determinant and thus they concluded that dynamic electron correlation, rather than nondynamic correlation, is the most important effect in reproducing the Fe–Cp distance. Almlof and his co-workers have, therefore, found that the MP2 calculations produced a better metal–ligand distance, within 0.08 Å of the experimental value, than the HF calculations.[16] A more accurate wave function, than perturbation theory, would be required to obtain more reasonable bond distances, whereas the quality of the basis function is less significant, as seen in the cases of $Fe(CO)_5$ and ferrocene.[13–16] A better wave function requires much more computational time, and thus we did not try to get structures closer to experiment with a better wave function. The orders in stability among products is expected not to be influenced by wave function, as will be seen in the small difference in relative stability between HF and MP2.

We have also carried out the harmonic vibrational analysis at the HF level. Since Fe–ligand bond distances are not reliable at the HF level, we discuss mainly the frequencies for CO stretching.

Results and Discussion

$[(\eta^5\text{-}C_5H_5)Fe(CO)_3]^+$ (I). Table I contains the optimized geometries of two conformations of $[(\eta^5\text{-}C_5H_5)Fe(CO)_3]^+$, with C_s symmetry, at the RHF/HUZ 3-21G level. The eclipsed and staggered conformers are denoted I_{ec} and I_{st}, respectively. The structure of I_{ec} is schematically shown in Figure 1. Also presented in the table are the optimized geometries of the eclipsed conformer at the RHF/HUZ 3-21G* level and at the RMP2/HUZ 3-21G level. Table I also contains the total energies as well as the RHF/HUZ 3-21G relative energies.

At first, we discuss the geometrical parameters obtained using the RHF method. By comparison of the RHF/HUZ 3-21G results for the conformers I_{ec} and I_{st}, it can be seen that the geometries and energies of the two conformers differ little. This is in agreement with the results of Hoffmann and co-workers, who calculated a rotation barrier between the two conformers of 0.002 kcal/mol at

---

(11) Albright, T. A.; Hofmann, P.; Hoffmann, R. *J. Am. Chem. Soc.* **1977**, *99*, 7546.

(12) Elian, M.; Hoffmann, R. *Inorg. Chem.* **1975**, *14*, 1058.

(13) Almlof, J.; Luthi, H. P.; Seigbahn, P. E. M. *J. Phys. Chem.* **1985**, *89*, 2156.

(14) Almlof, J.; Faegri, K.; Luthi, H. P.; Ammeter, J. H.; *J. Chem. Phys.* **1982**, *77*, 2002.

(15) Luthi, H. P.; Almlof, J.; Faegri, K.; Schilling, B. E. R. *Chem. Phys. Lett.* **1984**, *106*, 266.

(16) Park, C.; Almlof, J. *J. Chem. Phys.* **1991**, *95*, 1829.

(17) (a) Barnes, L. A.; Rosi, M.; Bauschlicher, C. W. *J. Chem. Phys.* **1991**, *94*, 2031. (b) Ziegler, T.; Tschinke, V.; Ursenbach, C. *J. Am. Chem. Soc.* **1987**, *109*, 4825. (c) McKee, M. L. *J. Phys. Chem.* **1992**, *96*, 1683.

(18) (a) Dedieu, A.; Nakamura, S.; Sheldon, J. C. *Chem. Phys. Lett.* **1987**, *141*, 323. (b) Dedieu, A.; Nakamura, S. *Nouv. J. Chem.* **1984**, *8*, 317.

(19) *Gaussian 90*; Frisch, M. J., Head-Gordon, M., Trucks, G. W., Foresman, J. B., Schlegel, H. B., Raghavachari, K., Robb, M. A., Binkley, J. S., Gonzalez, C., Defrees, D. J., Fox, D. J., Whiteside, R. A., Seeger, R., Melius, C. F., Baker, J., Martin, R. L., Kahn, L. R., Stewart, J. J. P., Topiol, S., Pople, J. A., Eds.; Gaussian, Inc.; Pittsburgh PA, 1990.

(20) Huzinaga, S. *Gaussian Basis Sets for Molecular Calculations*; Elsevier, New York, 1984.

Table I. Optimized Geometries of $[(\eta^5\text{-}C_5H_5)Fe(CO)_3]^+$ in Eclipsed, I_{ec}, and Staggered, I_{st}, Conformations[a]

	I_{ec} RHF/HUZ 3-21G	I_{ec} RHF/HUZ 3-21G*	I_{ec} RMP2/HUZ 3-21G	I_{st} RHF/HUZ 3-21G
Fe–C_x	2.122	2.153	1.658	2.117
Fe–C_y	2.119	2.148	1.657	2.121
O_x–C_x	1.118	1.102	1.192	1.117
O_y–C_y	1.118	1.102	1.193	1.118
Fe–C_1	2.272	2.278	2.030	2.228
Fe–C_2	2.235	2.245	2.042	2.269
Fe–C_3	2.261	2.268	2.034	2.248
H_1–C_1	1.069	1.075	1.082	1.067
H_2–C_2	1.067	1.074	1.083	1.069
H_3–C_3	1.068	1.075	1.082	1.068
C_xFeZ	58.17	57.81	55.79	58.17
C_yFeZC_x	119.56	119.53	120.00	120.39
O_xC_xFe	175.48	175.72	177.06	175.51
O_yC_yFe	175.40	175.50	177.27	175.33
O_yFeZC_x	119.56	119.47	119.90	120.52
C_1FeZ	147.62	148.14	142.09	146.53
C_2FeZ	147.08	147.41	142.49	147.76
C_3FeZ	147.06	147.96	142.89	147.91
C_1FeZC_x	(0.0)	(0.0)	(0.0)	(180.0)
C_2FeZC_x	71.09	71.73	71.46	108.52
C_3FeZC_x	144.13	144.44	143.64	37.04
H_1C_1Fe	124.65	123.35	128.23	128.12
H_2C_2Fe	127.61	126.43	125.52	124.94
H_3C_3Fe	125.71	124.37	127.23	126.71
H_2FeZC_x	71.50	71.78	71.67	108.29
H_3FeZC_x	144.06	144.27	143.87	36.55
E	−1789.291 869	−1789.727 563	−1790.768 566	−1789.291 867
ΔE	0.0			0.00

[a] The staggered conformer is formed by rotating the C_5H_5 ring 180° prior to optimization. (Bond lengths are in Å, bond angles in deg.) Total energies (in au) and relative energies (in kcal/mol) are included.

Table II. Selected Vibrational Frequencies (in cm^{-1}) of Stationary Points Determined at the RHF/HUZ 3-21G Level

species I_{ec}				species I_{st}			
ν_6	a′	2430	sym CO str	ν_6	a″	2430	sym CO str
ν_7	a″	2428	asym CO str	ν_7	a′	2428	asym CO str
ν_8	a′	2427	asym CO str	ν_8	a′	2427	asym CO str
ν_{42}	a″	6i	Cp ring rotn wrt $Fe(CO)_3$	ν_{42}	a″	9.8i	Cp ring rotn wrt $Fe(CO)_3$
species II				species III_{ecH}			
ν_6	a′	2364	CO str	ν_7	a′	2389	CO str
ν_7	a″	2357	CO str	ν_8	a″	2386	CO str
ν_8	a′	2334	CO str	ν_9	a′	1716	formyl CO str
ν_9	a′	1649	Fe–H str	ν_{48}	a″	28i	formyl group rotn around Fe–C_x bond
species III_{ecO}				species III_{stH}			
ν_7	a′	2379	CO str	ν_7	a′	2389	CO str
ν_8	a″	2376	CO str	ν_8	a″	2386	CO str
ν_9	a′	1772	formyl CO str	ν_9	a′	1715	formyl CO str
				ν_{47}	a″	14i	Cp ring rotn wrt $Fe(CO)_3$
				ν_{48}	a″	24i	formyl group rotn around Fe–C_x bond
species IV_{ec}				species IV_{st}			
ν_7	a′	2336	sym CO str	ν_7	a′	2338	sym CO str
ν_8	a″	2327	asym CO str	ν_8	a′	2249	asym CO str
ν_9	a′	2320	asym CO str	ν_9	a″	2215	asym CO str
				ν_{48}	a″	325	C_5H_6 ring rotn wrt $Fe(CO)_3$

the extended Hückel level.[11] A vibrational frequency analysis carried out on each conformer, shown in Table II, gave a small imaginary frequency in each case, 9.8*i* cm^{-1} in I_{st} and 6.0*i* cm^{-1} in I_{ec}, corresponding to ring rotations. For an ideal pentagonal structure of the C_5H_5 ring, the difference between the eclipsed and staggered forms is the rotation of the C_5H_5 ring by 36°. The imaginary frequencies for both conformers suggest that the rotation angle at the real minimum would be about 18°, out of C_s symmetry. However, the small magnitudes of the imaginary frequencies also suggest that the energy change with respect to the rotation is small. Accordingly, we have not studied further the conformation of the C_5H_5 ring. The similarity in geometry and energy of the two conformers indicates that the effect of rotating the C_5H_5 ring is minimal. Thus in this work attention is focused on the experimentally known eclipsed conformer.[21]

RHF average bond parameters obtained using the HUZ 3-21G* basis set and those obtained using the smaller HUZ 3-21G basis set, as well as experimental values, are summarized in Table III for the eclipsed conformer. It can be seen that both HF calculations overestimate Fe–

---

[21] Gress, M. E.; Jacobson, R. A. *Inorg. Chem.* **1973**, *12*, 1746.

Table III. Average Optimized Parameters for the Eclipsed Conformers of $[(\eta^5\text{-}C_5H_5)Fe(CO)_3]^+$ and Experimental Values[21] (Bond Lengths in Å, Bond Angles in deg)

	RHF/ HUZ 3-21G	RHF/ HUZ 3-21G*	RMP2/ HUZ 3-21G	exptl
$Fe\text{-}CO_{av}$	2.120	2.150	1.657	1.816
$C\text{-}O_{av}$	1.118	1.102	1.193	1.112
$Fe\text{-}CC_{av}$	2.253	2.261	2.036	2.070
$FeCO_{av}$	175.43	175.58	177.20	177.27

CO and Fe–CC bond lengths. The RHF/HUZ 3-21G calculation overestimates the Fe–CO bond length by 17% and the Fe–CC bond length by 9%. Addition of d polarization functions on the C and O atoms makes the agreement with experiment worse. The effect of the added function is larger on the Fe–CO bond length.

The FeCO angle calculated with and without polarization functions agrees with the experiment. The calculated values are, in both cases, less than 2° smaller than the experimental values.

The C–C distances in the Cp ring are from 1.402 to 1.436 Å and the Fe–CC distances are from 2.235 to 2.272 Å at the RHF/HUZ 3-21G level. These results suggest that all the carbon atoms in the Cp ring interact with Fe to a similar extent.

The calculated RHF harmonic vibrational frequencies are summarized in Table II. The calculated ν_{CO} values in I are 2430 cm^{-1} (a′), 2428 cm^{-1} (a″), and 2427 cm^{-1} (a′). The calculated frequencies of I differ from the experimental values of 2127 and 2070 cm^{-1} for $[(\eta^5\text{-}C_5H_5)Fe(CO)_3]BF_4$ in Nujol mull.[22] Usually, RHF calculations overestimate experimental fundamental vibrational frequencies, because (1) the RHF method is too steep for dissociation and (2) anharmonicity is not taken into account. The empirical scale factor, which adjusts the calculated frequencies to experimental ones, is about 0.89 for organic molecules at the HF/3-21G level.[23] We find that the average scale factor for ν_{CO} of I is 0.86. Presumably, the correlation effect, which enhances back-donation and thus weakens the CO bonds, is more important in this first row transition metal complex than in organic molecules.

It is seen from Table III that using the RMP2 method improves the agreement between calculated and experimental geometries, compared to using the RHF method. The improvement in the Fe–C bond distances is noteworthy. The RMP2 calculations now underestimate the Fe–CO bond distances by 9% and the Fe–CC bond distance by less than 2%. Thus the Fe–CC average bond distance is improved more than the Fe–CO average bond distance. However the C–O bond length is now overestimated by 0.081 Å. The short Fe–CO and the long CO bond suggest that the back-donation at the RMP2 level is overestimated. The FeCO bond angle in the RMP2 case agrees almost exactly with the experimental value. In a detailed study of ferrocene by Park and Almlof[16] it was noted that the metal to ligand distance, calculated from MP2 calculations, with different basis sets, varied by only 0.01 Å. Thus, changing the basis sets considered at the MP2 level did not significantly alter the ferrocene geometry and the smallest basis set used was adequate. Our basis set is of almost comparable quality to the smallest one of Park and Almlof. Thus the basis set we use, within the MP2 method, is appropriate.

Table IV. Optimized Geometry of $[(\eta^5\text{-}C_5H_5)Fe(CO)_3H]$ and $[(\eta^3\text{-}C_5H_5)Fe(CO)_3H]$ (Bond Lengths in Å, Bond Angles in deg)[a]

	$[(\eta^5\text{-}C_5H_5)Fe(CO)_3H]$		$[(\eta^3\text{-}C_5H_5)Fe(CO)_3H]$
	RHF/ HUZ 3-21G	RMP2/ HUZ 3-21G[b]	RMP2/HUZ 3-21G
$Fe\text{-}C_x$	4.332	4.146	1.683
$Fe\text{-}C_y$	2.064	1.614	1.648
$O_x\text{-}C_x$	1.127	1.172	1.212
$O_y\text{-}C_y$	1.125	1.207	1.199
$H_x\text{-}Fe$	1.641	1.397	1.437
$Fe\text{-}C_1$	2.322	2.002	1.936
$Fe\text{-}C_2$	2.302	2.039	2.038
$Fe\text{-}C_3$	2.309	2.014	2.954
$H_1\text{-}C_1$	1.067	1.080	1.078
$H_2\text{-}C_2$	1.067	1.057	1.083
$H_3\text{-}C_3$	1.069	1.081	1.082
C_xFeZ	50.182	49.40	116.57
H_xFeZ	61.431	67.93	55.66
C_yFeZC_x	74.00	71.60	71.60
O_xC_xFe	169.99	170.61	175.62
O_yC_yFe	172.68	179.31	176.39
O_yFeZC_x	77.36	71.35	69.80
C_1FeZ	159.16	149.03	155.28
C_2FeZ	150.14	144.38	119.28
C_3FeZ	139.75	135.78	100.59
C_1FeZC_x	(180.0)	(180.0)	(180.0)
C_2FeZC_x	91.07	98.08	141.17
C_3FeZC_x	28.10	31.15	166.63
H_1C_1Fe	120.83	128.49	124.30
H_2C_2Fe	124.57	115.39	117.46
H_3C_3Fe	123.63	126.58	144.69
H_2FeZC_x	98.88	96.33	118.05
H_3FeZC_x	31.45	32.89	159.35
E	−1790.011 625	−1791.505 207	−1791.494 415

[a] Total energies (in au) are included. [b] Stopped at a maximum force of 0.04 au/radian.

$[(\eta^5\text{-}C_5H_5)Fe(CO)_3H]$ (II). Table IV shows the optimized geometry of $[(\eta^5\text{-}C_5H_5)Fe(CO)_3H]$ (II) at the RHF/HUZ 3-21G level. In this species the hydride H is staggered with respect to the carbon atoms in the Cp ring and one carbonyl group is in the C_s plane, as shown in Figure 1. In II all the calculated frequencies, shown in Table II, are positive, indicating that the C_s symmetric structure is a local minimum, different from I. The optimized structure shows that II is a weak complex, $[(\eta^5\text{-}C_5H_5)Fe(CO)_2H]\cdots CO$, with a Fe···CO distance of 4.332 Å. As in the parent cation, I, the C_5H_5 ring remains approximately planar in II. The Fe–CC distances range from 2.302 to 2.322 Å. These values are slightly larger than in I.

In II the shorter Fe—CO distance is 2.064 Å and the average C—O bond length is 1.126 Å. These may be compared with the corresponding values of 2.120 and 1.118 Å in I. Thus the Fe—CO distance decreases and the C—O distance increases in going from I to II. Adding a hydride to I is expected to make the iron atom less positive, increase back-donation to the carbonyls, and decrease Fe—CO and increase C–O bond lengths, making ν_{CO} smaller, corresponding to $Fe\text{—}C\equiv O$ contributing to a greater extent in I and $Fe=C=O$ to II. In I the iron charge, based on a Mulliken population analysis, was calculated to be 0.70 and in II 0.43, in conformity with the above argument. The shorter Fe—CO bond in II is as expected, as is the longer C—O bond distance. Thus the above arguments agree with calculations. The calculated ν_{CO} values in II are 2364 cm^{-1} (a′), 2357 cm^{-1} (a″), and 2334 cm^{-1} (a′), which are smaller than those for I. The change to lower frequencies is as expected.

The RMP2 geometry optimization for II was stopped before complete convergence (maximum force = 0.04 au/

---

[22] Kochhar, R. K.; Pettit, R. *J. Organomet. Chem.* **1966**, *6*, 272.

[23] Pople, J. A.; Schlegel, H. B.; Krishnan, R.; Defrees, D. J.; Binkley, J. S.; Frisch, M. J.; Whiteside, R. A.; Hout, R. F.; Hehre, W. J. *Int. J. Quantum Chem. Quantum Chem. Symp.* **1981**, *15*, 269.

Table V. Optimized Geometries of Conformers of [(η^5-C_5H_5)Fe(CO)$_2$CHO] (Bond Lengths in Å, Bond Angles in deg)[a]

	III$_{ecH}$ RHF/HUZ 3-21G	III$_{ecH}$ RMP2/HUZ 3-21G	III$_{stH}$ RHF/HUZ 3-21G	III$_{ecO}$ RHF/HUZ 3-21G
Fe–C$_x$	2.048	1.890	2.048	2.057
Fe–C$_y$	2.110	1.611	2.112	2.086
O$_x$–C$_x$	1.243	1.237	1.243	1.230
O$_y$–C$_y$	1.122	1.208	1.122	1.123
H$_x$–C$_x$	1.106	1.106	1.105	1.123
Fe–C$_1$	2.313	2.028	2.284	2.279
Fe–C$_2$	2.297	2.031	2.318	2.271
Fe–C$_3$	2.312	2.012	2.312	2.309
H$_1$–C$_1$	1.068	1.082	1.068	1.066
H$_2$–C$_2$	1.068	1.082	1.069	1.068
H$_3$–C$_3$	1.069	1.081	1.067	1.069
C$_x$FeZ	52.20	54.10	52.12	56.14
H$_x$C$_x$Fe	128.11	113.08	128.19	121.94
C$_y$FeZC$_x$	114.88	117.08	115.37	115.79
O$_x$C$_x$Fe	115.85	126.98	115.75	123.35
O$_y$C$_y$Fe	179.93	176.79	180.09	178.71
O$_y$FeZC$_x$	112.91	118.77	113.48	113.47
C$_1$FeZ	152.15	141.11	143.99	148.23
C$_2$FeZ	149.77	141.92	147.29	147.92
C$_3$FeZ	145.77	143.28	151.76	148.43
C$_1$FeZC$_x$	(0.0)	(0.0)	(180.0)	(0.0)
C$_2$FeZC$_x$	77.19	69.80	113.79	71.86
C$_3$FeZC$_x$	147.31	142.90	40.75	144.51
H$_1$C$_1$Fe	121.36	127.66	125.93	116.74
H$_2$C$_2$Fe	124.90	126.80	123.20	124.64
H$_3$C$_3$Fe	124.06	127.21	123.48	125.12
H$_2$FeZC$_x$	74.79	70.69	111.17	71.84
H$_3$FeZC$_x$	145.87	143.36	38.40	144.30
E	−1790.015 041	−1791.496 925	−1790.014 832	−1790.006 351
ΔE	0.0		0.1	5.5

[a] Total energies (in au) and relative energies (in kcal/mol) are included.

radian), since the results obtained show the same pattern, a weak [(η^5-C_5H_5)Fe(CO)$_2$H]···CO complex, as do the HF results. The results are summarized in Table IV.

[(η^3-C_5H_5)Fe(CO)$_3$H] (V). While in II one CO group binds to the Fe complex weakly, it is expected that this CO group may coordinate to the Fe atom directly with C_5H_5 ring slippage from η^5 to η^3, as η^3 complexes with the C_5H_5 ring bent out of plane are known.[24] Therefore, we undertook a detailed specific search for the [(η^3-C_5H_5)-Fe(CO)$_3$H] species at the RMP2 level. The structural parameters are shown in Table IV. V is less stable than II and in fact less stable than all other products resulting from the hydride attack considered. It is interesting to note that in the allyl moiety one optimized Fe–C distance is 1.936 Å and the other distances are 2.038 Å, while the remaining Fe–C(ring) distances are both 2.954 Å. In the allyl moiety the CC distances are 1.467 Å, and in the olefin moiety the CC distance is 1.343 Å, close to the CC distance in free ethylene. The distances for the CC bonds connecting the allyl and olefin moieties are 1.574 Å, which is similar to that of the CC single bond. These structural features show that C_5H_5 ring slippage takes place to lead to η^3 coordination through the allyl moiety and the olefin moiety is intact. The Fe–C(O) distance for the carbon in the C_s plane is 1.683 Å, while the other Fe–C(O) distances are 1.648 Å. Thus, as expected, there is not any long Fe–C(O) distance as seen in II.

[(η^5-C_5H_5)Fe(CO)$_2$CHO] (III). In Table V the geometries and the total and relative energies of three conformers of [(η^5-C_5H_5)Fe(CO)$_2$CHO] (III) are shown. These are termed III$_{ecH}$, in which C$_1$, H$_1$, Fe, C$_x$, O$_x$, and H$_x$ are in the C_s plane and H$_x$ is close to the C_5H_5 ring and eclipses C$_1$, as shown in Figure 1, III$_{stH}$, in which the ring is rotated by 180°, and III$_{ecO}$, in which the CHO group in III$_{ecH}$ is rotated by 180° about the Fe–C$_x$ axis.

By comparison of the RHF geometry of I$_{ec}$ and that of the lowest energy form of [(η^5-C_5H_5)Fe(CO)$_2$CHO], III$_{ecH}$, it is noted that the Fe—C$_y$ bond distance in the metal—formyl species is shorter than in I and that the corresponding C—O bond distance is longer. Thus Fe═C═O contributes to a greater extent in III. This is as expected, since in I there is back-donation from iron to three carbonyl groups and in III the back-donation is to two carbonyl groups only and thus is greater. Also, in the neutral III the back-donation can take place more strongly than in the cationic I. This result is reflected in the ν_{CO} values, calculated at the HF level, shown in Table II, which are 2389 cm^{-1} (a′) and 2386 cm^{-1} (a″) in III$_{ecH}$, while the corresponding values in I$_{ec}$ are 2430 cm^{-1} (a′), 2428 cm^{-1} (a″), and 2427 cm^{-1} (a′). The experimental results also agree with the calculated trends, since in III[25] the carbonyl stretching frequencies are 2026 and 1969 cm^{-1} and in I[22] they are 2127 and 2070 cm^{-1}. The required average scale factor for carbonyl stretching in III is 0.84, similar to that for I. The unscaled calculated CO stretch in the formyl group in III$_{ecH}$ is at 1716 cm^{-1}. This is appreciably less than the calculated carbonyl stretching frequencies, as expected.

Considering the RHF energies of the three conformers of III, there is little energy difference between III$_{ecH}$ and III$_{stH}$ (Table V), as expected. The eclipsed form is slightly more stable. Also III$_{ecH}$ has less destabilization than III$_{ecO}$ (5.5 kcal/mol), since it has the small hydrogen close to the C_5H_5 ring. (The O$_x$–C$_1$ distance in III$_{ecO}$ is 3.771 Å and the H$_x$–C$_1$ distance is 3.432 Å in III$_{ecH}$.)

The least stable conformer, III$_{ecO}$, has no imaginary frequencies and is thus a true local minimum. However

---

[24] Huttner, G.; Brintzinger, H. H.; Bell, L. G.; Friedrich, P.; Bejenke, V. *J. Organomet. Chem.* 1978, *145*, 329.

[25] Ahmed, H. Ph.D. Thesis, NUI, 1991.

the most stable conformer, III_{ecH}, has a small imaginary frequency at 28i cm^{-1}, indicating a tendency to rotate slightly the formyl group around the Fe–C_x bond, deviating from C_s symmetry. In the most stable III_{ecH} the rotation would reduce the small steric repulsion between the formyl hydrogen and the C_5H_5 ring. Thus the true minimum would be located at a nonzero value of θ, the rotation angle, with $\theta = 0°$ for ecH and $\theta = 180°$ for ecO. At the region around ecO, a destabilizing steric interaction between the formyl oxygen and the C_5H_5 ring takes place, to make III_{ecO} the least stable of the three conformers considered. In this region, however, the hydrogen bonding between the formyl oxygen O_x and a cyclopentadienyl hydrogen H_1 takes place at the O_xH_1 distance of 2.6 Å, resulting in the local minimum, and preserves C_s symmetry in III_{ecO}.

Conformer III_{stH} has two small imaginary frequencies of 24i and 14i cm^{-1}. One of these corresponds to the formyl group rotation which is similar to that discussed above for III_{ecH}. The other shows that III_{stH} is the least stable rotamer with respect to the C_5H_5 ring rotation. The small imaginary frequency of 14i cm^{-1} and the small energy difference between III_{ecH} and III_{stH} show that the C_5H_5 ring can rotate almost freely. In III_{stH} the two carbonyl groups (C_yO_y) approximately eclipse the C_3–H moieties of the C_5H_5 ring. Thus this conformer, III_{stH}, is sterically slightly less stable than III_{ecH}. The smaller H is closer to the C_5H_5 ring than the larger O, stabilizing III_{stH} relative to III_{ecO}.

Thus, III_{ecH} is the most stable of the three conformers (Table V), due to less steric repulsions, as noted above. For this conformer of [(η^5-C_5H_5)Fe(CO)$_2$CHO] geometry optimized RMP2 calculations were undertaken. A comparison of the RMP2 bond lengths of the FeCO moieties in I and III reveal the expected pattern, since III has the shorter Fe–CO and longer C–O bond distances, as discussed for II at the RHF level.

By comparison of the RMP2 and RHF calculations in III_{ecH}, it is noted that the Fe–CO bond distance is 0.499 Å shorter at the RMP2 level. A similar contraction occurred in I_{ec}. However in III_{ecH} the Fe–CHO bond distance does not show such a contraction; the contraction in going from the RHF to the RMP2 calculations is 0.158 Å in this case. In addition, the correlation effect decreases the C(H)–O bond distance in III_{ecH} by 0.006 Å and increases the carbonyl C–O distance by 0.086 Å. Thus in the RMP2 calculations on III_{ecH}, the correlation effect alters the Fe–CO and FeC–O bond distances more than the Fe–C(H)O and FeC(H)–O ones. The carbonyl groups have two π^* orbitals, while the formyl group has only one. Therefore, enhancement of back-donation at the RMP2 level affects the Fe–CO and FeC–O bond distances more. It is noteworthy that at the RHF level the Fe–CHO bond length is less than the Fe–CO one, while at the RMP2 level the Fe–CHO bond length is appreciably larger than the Fe–CO distance. This is an important point, since the RMP2 trend is in agreement with the traditional concept of bonding in metal carbonyl complexes. Thus, taken together, these effects show that the metal to carbonyl back-bonding is poorly described at the HF level, even though the ν_{CO} frequency changes at the RHF level correlate with the experiment.

[(η^4-C_5H_6)Fe(CO)$_3$] (IV). Two extreme models of interactions between metal and tetrahapto ligands (η^4) may be considered, one of which (a) has two independent η^2-alkene–metal bonds while in the other (b) there are two σ bonds from the extremities and one η^2-alkene–metal bond from the center of the diene. Mingos[26,27] has discussed a simplified molecular orbital model for η^4-diene metal complexes, e.g. [(η^4-C_4H_6)Fe(CO)$_3$], where the two most important interactions are donation from a butadiene $1\pi_a$ occupied orbital to a [Fe(CO)$_3$] $2e_a$ unoccupied orbital and back-donation from the [Fe(CO)$_3$] $2e_s$ occupied orbital to the butadiene $2\pi_s$ unoccupied orbital. These forward and back donations have a tendency to equalize the C–C bond distances in the butadiene moiety. The standard experimental distances are 1.404 and 1.419 Å for inner and outer CC bonds of the diene moiety in 1,3-diene tricarbonyliron complexes. Mingos noted that in general the unique carbonyl in these complexes points away from the butadiene moiety, to maximize overlap. Hoffmann and Hofmann[28] discussed the bonding in cyclobutenyl transition metal complexes along similar lines.

Table VI summarizes the geometries and total energies of the conformers of IV considered. Firstly, the results obtained by the HF method are discussed as done previously. We determined the structures of the two conformers at the RHF level, IV_{ec} and IV_{st}. IV_{ec} has the carbonyl group in the C_s plane, eclipsing the carbon of CH_2 also in the C_s plane, as shown in Figure 1, while in IV_{st} the ring is rotated 180°. The RHF/HUZ 3-21G calculations showed that IV_{ec} is 25.4 kcal/mol more stable than IV_{st}, in agreement with the prediction of Mingos noted above. However, as dicussed in the Method of Calculation, the RHF wave function of IV is unstable with respect to becoming the UHF wave function and in such a case the RHF optimized structure is not reliable.

Actually, the RHF calculation favors bonding model b, in disagreement with the experimental structures for 1,3-diene complexes mentioned above; (i) while the single CH—CH_2 bond length is 1.550 Å, the bond lengths, within the conjugated carbon chain, are 1.472 Å for the outer C_2—C_3 bond and 1.381 Å for the inner C_3—C_3 bond, indicating a C_3=C_3 double bond, (ii) the Fe—C_2 distances of 2.094 Å in IV_{ec} are much shorter than the Fe—$C_{1,2,3}$ distances in I–III, indicating the existence of two Fe—C_2 σ bonds, and (iii) the short Fe—C_3 distances of 2.19 Å in IV_{ec} also suggest that the inner C_3=C_3 double bond interacts strongly with the Fe atom. Also, the rotation barrier of 25.4 kcal/mol is overestimated, compared with the experimental value of 9.5 kcal/mol for the analogous (butadiene)Fe(CO)$_3$ complex.[29]

Thus we performed at the UHF/HUZ 3-21G level the geometry optimization for IV_{ec}, which is more stable at the RHF level and corresponds to the experimental structures for 1,3-diene tricarbonyliron complexes with the endo inner bond. The result is shown in Table VI. The UHF calculations gave a square pyramidal structure with two C_2C_3 bonds and two C_yO_y groups in the basal plane and C_xO_x in the apical position. In this UHF structure both inner and outer CC bond distances of the diene moiety are 1.417 Å, close to the experimental structures of the 1,3-diene tricarbonyliron complexes mentioned above.[30] As discussed in the beginning of this section, an equalization of the CC bond distances is the result of strong donation and back-donation.

---

[26] Mingos, D. M. P. *J. Chem. Soc., Dalton Trans.* **1977**, 20.

[27] Mingos, D. M. P. In *Comprehensive Organometallic Chemistry*; Wilkinson, G., Stone, F. G. A., Abel, E. A., Eds.; Pergamon Press: Oxford, U.K., 1982; Vol. 3, p 1.

[28] Hoffmann, R., Hofmann, P. *J. Am. Chem. Soc.* **1976**, *98*, 598.

[29] Kruczynski, L.; Takats, J. *J. Am. Chem. Soc.* **1974**, *96*, 932.

[30] Cotton, F. A.; Day, V. W.; Frenz, B. A.; Hardcastle, K. I.; Troup, J. M. *J. Am. Chem. Soc.* **1973**, *95*, 4522.

Table VI. Optimized Geometries of Conformers of $[(\eta^4\text{-}C_5H_6)Fe(CO)_3]$ (Bond Lengths in Å, Bond Angles in deg)[a]

	IV$_{ec}$ RHF/HUZ 3-21G	IV$_{ec}$ UHF/HUZ 3-21G	IV$_{ec}$ RMP2/HUZ 3-21G	IV$_{st}$ RHF/HUZ 3-21G
Fe–C$_x$	1.978	2.257	1.758	1.971
Fe–C$_y$	2.026	2.057	1.652	1.962
O$_x$–C$_x$	1.128	1.128	1.210	1.126
O$_y$–C$_y$	1.127	1.142	1.210	1.135
Fe–C$_1$	2.628	2.770	2.712	2.773
Fe–C$_2$	2.094	2.360	2.180	2.239
Fe–C$_3$	2.190	2.253	1.999	2.150
H$_a$–C$_1$	1.095	1.097	1.103	1.099
H$_b$–C$_1$	1.083	1.081	1.086	1.079
H$_2$–C$_2$	1.075	1.070	1.083	1.072
H$_3$–C$_3$	1.072	1.069	1.081	1.070
C$_x$FeZ	62.37	54.44	56.36	62.99
C$_y$FeZC$_x$	118.28	125.67	124.89	123.92
O$_x$C$_x$Fe	171.36	171.84	169.15	176.87
O$_y$C$_y$Fe	171.44	174.07	175.24	173.74
O$_y$FeZC$_x$	116.33	125.73	123.85	124.91
C$_1$FeZ	144.95	131.00	131.52	145.74
C$_2$FeZ	141.95	136.53	134.52	143.79
C$_3$FeZ	152.10	161.23	156.47	152.19
C$_1$FeZC$_x$	(0.0)	(0.0)	(0.0)	(180.0)
C$_2$FeZC$_x$	62.16	46.67	47.47	120.16
C$_3$FeZC$_x$	137.63	102.28	110.11	46.19
H$_a$C$_1$Fe	151.41	156.64	148.35	152.19
H$_b$C$_1$Fe	100.27	95.86	101.11	99.14
H$_2$C$_2$Fe	136.41	129.71	120.26	128.98
H$_3$C$_3$Fe	125.01	118.12	121.08	121.99
H$_2$FeZC$_x$	71.07	57.27	58.19	113.50
H$_3$FeZC$_x$	129.26	126.74	128.63	40.98
E	−1789.979 368	−1790.008 173	−1791.623 845	−1789.938 856
ΔE	0.0			25.4

[a] Total energies (in au) and relative energies (in kcal/mol) are included.

Table VII. Total Energies (in au) and Relative Energies (in kcal/mol) of the Species Considered Compared to I$_{ec}$ + H$^-$, Using the HUZ 3-21G Basis Set

		E	ΔE		E	ΔE
I + H$^-$	RHF[a]	−1789.692 29	0	RMP2[c]	−1791.174 94	0
II	RHF[a]	−1790.011 63	−200	RMP2[c]	−1791.505 21	−207
III	RHF[a]	−1790.015 04	−203	RMP2[c]	−1791.496 93	−202
IV	UHF[b]	−1790.008 17	−198	RMP2[c]	−1791.623 85	−282
	PUHF[b]	−1790.027 36	−210	UMP2[c]	−1791.483 83	−194
				PUMP2[c]	−1791.540 59	−230
V				RMP2[c]	−1791.494 42	−200

[a] At RHF geometry. [b] At UHF geometry. [c] At RMP2 geometry.

Note that at the UHF level the Fe–CO distances of 2.257 and 2.057 Å are very long, as expected. The UHF wave function shows that with this weak ligand field the iron atom has two parallel spins which induce the spin-flipping on the diene moiety. As a result, electronic states up to a septet may contaminate the wave function. In fact, a large expectation value of S^2 of 2.3542 was calculated for the UHF wave function. Therefore these contaminations have to be projected out, in order to obtain the correct energy. Thus the PUHF calculations with spin projection up to a nonet were carried out. The UHF energy for the UHF structure was 18 kcal/mol lower than the RHF energy for the RHF structure, while upon spin projection a further stabilization by 12 kcal/mol was obtained. As a result at the HF level IV is the most stable among the products considered, as shown in Table VII.

If the contributions of the open-shell electronic structures are small enough, the RMP2 calculation would recover those contributions. Therefore, we determined the structure of IV at the RMP2 level with the HUZ 3-21G basis set. The RMP2 optimized C–C bond distances in the conjugated system are of interest. The outer C–C bond lengths are 1.416 Å, and the inner one is 1.499 Å, while the CH–CH$_2$ bond length is 1.531 Å. Thus the RMP2 calculations favor bonding model a based on butadiene coordinated through two η^2-moieties, which differs from the UHF as well as RHF results. Thus one could consider the RMP2 bonding as due to 1,3-cyclopentadiene coordinated to Fe(CO)$_3$. The RHF calculation is unable to describe the Fe–olefin bonding interaction properly, as seen in the theoretical treatment of the Fe–Cp bonding. As a result, the Fe–olefin coordination energy would be underestimated at the RHF level. Therefore, the RHF calculations artificially favor bonding model b. Finally, it is noted that, from the RMP2 calculations on I and IV, the latter has a longer average C–O bond distance but it also has a longer average Fe–CO distance. Presumably, electron donation from C$_5$H$_6$ suppresses electron donation from CO, which dominates Fe–CO interactions and is accompanied by back-donation.

The RMP2 calculation shows that IV is the most stable among the products; the energy of IV, relative to I + H$^-$, was calculated to be −282 kcal/mol. However, the RHF wave function for the RMP2 optimized structure is unstable too, resulting in overestimation of the correlation energy at the RMP2 level. Thus we carried out the PUMP2 energy calculation at the RMP2 optimized structure, in order to obtain a more reliable energy. The UHF wave function for the RMP2 structure has the expectation value of S^2 of 1.1146. The stronger ligand field due to the shorter Fe–CO distances, relative to those in the UHF optimized structure, decreases $\langle S^2 \rangle$. The PUMP2 energy, relative to I + H$^-$, is −230 kcal/mol. Removing spin contamination does not alter the fact that species IV has the greatest stability. At the MP2 level as well as the HF level, this result is only found when spin contamination is removed, as seen in Table VII.

We also considered the geometry determination at the UMP2 level. At the MP2 level, the lowest energy was obtained with the RMP2 wave function at the RMP2 structure, due to the overestimation of the correlation energy mentioned above. Thus, if we completed the UMP2 optimization, we would obtain a better structure and energy. However, the result that IV is the most stable would be unchanged. Therefore, we did not continue the UMP2 geometry determination.

Energy Comparisons. Table VII summarizes the relative energies of the lowest energy conformers considered. In the present calculation, an anion basis function, with a diffuse s function, was not used for the hydride anion and thus the energies relative to I + H^- are overestimated. However, comparison of the energies among the neutral II–IV, in which the energies are not much affected by the diffuse function, is the main issue. Therefore, we did not recalculate the energies with such an anion basis function.

In conclusion, the species formed by direct H^- attack on the metal (i.e. II) is at the MP2 level of energy similar to that of the metal–formyl (III) with the important result that, at the stable minimum of II, one of the Fe–CO bonds has been stretched to 4.146 Å. In other words, this species is a weak complex between the well-known hydride $[(\eta^5\text{-}C_5H_5)Fe(CO)_2H]$ and CO. Interestingly, the product corresponding to ring-slippage, $[(\eta^3\text{-}C_5H_5)Fe(CO)_3H]$ less stable than the other products, was detected. The metal–formyl species $[(\eta^5\text{-}C_5H_5)Fe(CO)_2CHO]$ is reasonably stable with respect to the isolated substrate cation (I) and hydride ion and so might well be expected to occur. Finally, the diene derivative, $[(\eta^4\text{-}C_5H_6)Fe(CO)_3]$ (IV), is considerably more stable than either of the metal or carbonyl attack products II and III and so, on the basis of these calculations, should be a thermodynamically stable product.

Comparison with Experiment

The formation of both the stable dimer $[(\eta^5\text{-}C_5H_5)Fe(CO)_2]_2$ and the diene complex $[(\eta^4\text{-}C_5H_6)Fe(CO)_3]$ (IV) under different reaction conditions led to early suggestions that ring attack and formation of IV occurred first in the reactions of $NaBH_4$ and I and that IV then rearranged to the hydride $[(\eta^5\text{-}C_5H_5)Fe(CO)_2H]$, which subsequently dimerized.[31,32] However, by the use of low temperature IR and NMR spectroscopy, we have shown that, using $NaBH_4$ in acetone at -80 °C, initial hydride attack occurs at a carbonyl atom to form the metal–formyl (III). When the temperature is raised to -20 °C, III loses a CO group to form the metal hydride $[(\eta^5\text{-}C_5H_5)Fe(CO)_2H]$. No spectroscopic evidence was obtained for the direct attack metal–hydride intermediate (II), in accord with the above theoretical results, which shows clearly that loss of CO tends to occur as this species forms. The observation of the formyl (III) at -80 to -20 °C is in excellent agreement with the calculated stability of III. Interestingly, in the reaction of the analogous indenyl system $[(\eta^5\text{-}C_9H_7)Fe(CO)_3]^+$ with BH_3CN^- at low temperatures, spectroscopic evidence was obtained for a ring-slipped analogue of II, i.e. $[(\eta^3\text{-}C_9H_7)Fe(CO)_3H]$.[10] In the present studies the ring-slippage analogue of II is at a higher energy than all the other hydride attack products. Reaction of I with $NaBD_4$ in acetone led to the analogous deuterated species, thereby proving that prior exo-ring attack and formation of IV with subsequent transfer of the endo-ring hydrogen to form $[(\eta^5\text{-}C_5H_5)Fe(CO)_2H]$ did not occur as previously postulated.

The calculated total energy (at MP2 level) of the diene complex (IV) shows that it is the most stable of the species considered theoretically in this paper, and the fact, therefore, that it is not observed during the low temperature studies with $NaBH_4$ suggests the existence of two reaction pathways, one at low temperatures, giving the kinetic products, $[(\eta^5\text{-}C_5H_5)Fe(CO)_2CHO] \rightarrow [(\eta^5\text{-}C_5H_5)Fe(CO)_2H] \rightarrow$ dimer, and a second higher temperature one leading to the ring product (IV). Presumably, for this pathway exo-ring attack involves the nucleophile (H^-), having overcome the repulsion energy between it and the π-electrons of the C_5H_5 ring, in contrast to the lower temperature pathways of direct attack at the metal or carbonyl group. Proof of these statements would require full reaction profile calculations, which are not feasible at the moment.

Finally, it should be stressed that the calculated energies in this paper apply to isolated simple hydride addition species in the gaseous phase. Solvent effects in these systems are quite marked, as are those due to varying the nature of the donor hydride.[33] For example, preliminary studies of the reactions of I with BH_3CN^- in THF at low temperatures have confirmed the formation of III, but in addition a formyl adduct, possibly $[(\eta^5\text{-}C_5H_5)Fe(CO)_2\text{-}CHO\cdot BH_2CN]$, is observed together with two hydride species, possibly II and the normal hydride $[(\eta^5\text{-}C_5H_5)Fe(CO)_2H]$.

Acknowledgment. N.J.F. and P.J.G. wish to thank IMS and UCD for making visits to Japan possible. The authors thank the Computer Centre, IMS, Okazaki National Research Institutes for the use of the HITAC M-680H and S-820/80 computers. Use of an IBM RS/6000 workstation in IMS is also acknowledged. The authors also acknowledge useful comments by referees.

OM920533J

---

[31] Sternberg, H. W.; Wender, I. *Proc. Conf. Coord. Chem. London, Chem. Soc. Spec. Publ.* **1959**, *13*, 35.

[32] Davison, A.; Green, M. L. H.; Wilkinson, G. *J. Chem. Soc.* **1961**, 3172.

[33] Brown, D. A.; Glass, W. K.; Ubeid, M. T. *Inorg. Chim. Acta* **1984**, *89*, L47.